The Outsized Role of Salps in Carbon Export in the Subarctic Northeast Pacific Ocean

Deborah K. Steinberg[1] , Karen Stamieszkin[1,2], Amy E. Maas[3] , Colleen A. Durkin[4] , Uta Passow[5] , Margaret L. Estapa[6], Melissa M. Omand[7] , Andrew M. P. McDonnell[8] , Lee Karp-Boss[9], Moira Galbraith[10] , and David A. Siegel[11]

[1]Department of Biological Sciences, Virginia Institute of Marine Science, William & Mary, Gloucester Point, VA, USA, [2]Bigelow Laboratory for Ocean Sciences, East Boothbay, ME, USA, [3]Bermuda Institute of Ocean Sciences, St. George's, Bermuda, [4]Monterey Bay Aquarium Research Institute, Moss Landing, CA, USA, [5]Ocean Sciences, Memorial University of Newfoundland, St John's, NL, Canada, [6]School of Marine Sciences, Darling Marine Center, University of Maine, Walpole, ME, USA, [7]Graduate School of Oceanography, University of Rhode Island, Narragansett, RI, USA, [8]College of Fisheries and Ocean Sciences, University of Alaska Fairbanks, Fairbanks, AK, USA, [9]School of Marine Sciences, University of Maine, Orono, ME, USA, [10]Department of Fisheries and Oceans, Institute of Ocean Sciences, Sidney, BC, Canada, [11]Earth Research Institute and Department of Geography, University of California Santa Barbara, Santa Barbara, CA, USA

Abstract Periodic blooms of salps (pelagic tunicates) can result in high export of organic matter, leading to an "outsized" role in the ocean's biological carbon pump (BCP). However, due to their episodic and patchy nature, salp blooms often go undetected and are rarely included in measurements or models of the BCP. We quantified salp-mediated export processes in the northeast subarctic Pacific Ocean in summer of 2018 during a bloom of *Salpa aspera*. Salps migrated from 300 to 750 m during the day into the upper 100 m at night. Salp fecal pellet production comprised up to 82% of the particulate organic carbon (POC) produced as fecal pellets by the entire epipelagic zooplankton community. Rapid sinking velocities of salp pellets (400–1,200 m d^{-1}) and low microbial respiration rates on pellets (<1% of pellet C respired day^{-1}) led to high salp pellet POC export from the euphotic zone-up to 48% of total sinking POC across the 100 m depth horizon. Salp active transport of carbon by diel vertical migration and carbon export from sinking salp carcasses was usually <10% of the total sinking POC flux. Salp-mediated export markedly increased BCP efficiency, increasing by 1.5-fold the proportion of net primary production exported as POC across the base of the euphotic zone and by 2.6-fold the proportion of this POC flux persisting 100 m below the euphotic zone. Salps have unique and important effects on ocean biogeochemistry and, especially in low flux settings, can dramatically increase BCP efficiency and thus carbon sequestration.

1. Introduction

Salps are pelagic tunicates that are ubiquitous throughout the world's oceans and their periodic blooms give rise to dense populations (Everett et al., 2011; Henschke et al., 2016; Madin et al., 2006; Stone & Steinberg, 2014). Their complex life cycle, with alternating sexual and asexual stages, provides the ability to rapidly respond to favorable environmental conditions. The resulting high abundances combined with some remarkable features of salp ecology and physiology can result in significant export of organic matter, potentially leading to an "outsized" role in the biological carbon pump (BCP) compared to other taxa. The high filtration rates of salps (Andersen, 1985; Madin & Cetta, 1984; Vargas & Madin, 2004) and the broad size spectrum of suspended particles they are able to consume (Ahmad Ishak et al., 2017; Stukel et al., 2021; Sutherland et al., 2010) result in effective packaging of small particles into large, rapidly sinking fecal pellets (Bruland & Silver, 1981; Madin & Deibel, 1998; Phillips et al., 2009). In addition, many salp species undergo extensive (hundreds of meters) diel vertical migration (DVM) (Madin et al., 1996, 2006; Stone & Steinberg, 2014; Wiebe et al., 1979), an adaptive behavior to avoid visual predators in sunlit-surface waters during the day. Feeding in surface waters at night and migrating to their mesopelagic residence depth during the day where their food is metabolized result in an "active transport" of carbon (Longhurst et al., 1990; Stone & Steinberg, 2016). Following the demise of a bloom, sinking salp carcasses are an additional export pathway, as evidenced by mass depositions of salps on the seafloor (Henschke et al., 2013; Lebrato et al., 2013; Smith et al., 2014).

It follows that when present, salps have the capacity to dominate export, particularly in low flux settings. The subarctic northeast Pacific Ocean is a high nutrient, low chlorophyll region where the food web is dominated by

small phytoplankton under tight grazer control by microzooplankton and mesozooplankton (Landry, Gifford, et al., 1993; Landry, Monger, & Selph, 1993) and <15% of net primary production (NPP) is exported below the euphotic zone (Buesseler & Boyd, 2009; Buesseler, Benitez-Nelson et al., 2020; Estapa et al., 2021). In such "retention" food webs, nutrients and organic material are retained and recycled in surface waters, with low export and potentially rapid flux attenuation (Buesseler & Boyd, 2009; Landry et al., 1995; Wassmann, 1997). "Export" food webs on the other hand, typical of highly productive periods or regions, are characterized by large phytoplankton and shorter food webs, with phytoplankton (e.g., diatoms) sinking out of the euphotic zone in aggregates, or grazed by larger zooplankton that enhance organic matter export through rapid sinking of their fecal pellets (Conroy et al., 2016; Michaels & Silver, 1988; Stukel et al., 2013; Wassmann, 1997). Salps are relatively large, generalist consumers that occur in both food web types and feed with mucous webs that can capture a wide size range of prey, including bacteria-sized particles (Stukel et al., 2021; Sutherland et al., 2010). Salps account for a high export of particulate organic carbon (POC) from surface waters to the deep sea through the flux of their large, fast-sinking fecal pellets (e.g., Phillips et al., 2009). Since these large zooplankton can feed at the base of the microbial food web on cyano- and other bacteria and export them in their feces (Pfannkuche & Lochte, 1993), even in an oligotrophic ecosystem state, they can short-circuit the material and energy flow in an otherwise retentive-type food web, increasing export appreciably. The presence of salps can have dramatic implications for export ratio and mesopelagic transfer efficiency of NPP, and ultimately carbon sequestration (Buesseler, Boyd, et al., 2020). However, salps are inherently patchy in space and time in part due to their ability to rapidly respond to favorable environmental conditions (Deibel & Paffenhöfer, 2009), making their contribution to exports poorly observed and constrained and thus rarely incorporated into models of the BCP.

While salp-mediated export processes—from fecal pellet production and vertical flux, to active transport via DVM, to carcass export—have been measured separately and modeled as an ensemble (Luo et al., 2020, 2022; Stone & Steinberg, 2016), these multiple processes are rarely measured in the field simultaneously (Wiebe et al., 1979). In the present study, we characterize the above full suite of salp-driven export processes during a bloom of *Salpa aspera* encountered in the subarctic Northeast Pacific Ocean in late summer as part of a research program investigating the BCP (EXport Processes in the Ocean from RemoTe Sensing [EXPORTS]) (Siegel et al., 2021) to quantify their collective role in export. Using this comprehensive sampling approach, we show that this single taxon can be responsible for dramatically increasing the transfer efficiency of the BCP in this otherwise retention-dominated food web.

2. Methods

2.1. Study Site and Sampling Scheme

Field sampling for this study took place in the subarctic northeast Pacific Ocean proximal to the Ocean Station Papa (OSP) time-series site (Station P; 145°W, 50°N) aboard the R/Vs *Roger Revelle* and *Sally Ride* from 14 August to 9 September 2018. An overview of the EXPORTS sampling plan, including context information on physical and bio-optical properties, nutrients, and phytoplankton biomass, is presented in Siegel et al. (2021). The study was conducted in three, 8-day repeating Lagrangian sampling cycles, or "epochs," tracking a neutrally buoyant float deployed at ~100 m depth. The epoch lengths were designed around three successive sediment trap deployments to capture sinking particles from the euphotic zone (Estapa et al., 2021). All sampling and experiments reported herein took place aboard the R/V *Revelle* "Process Ship," which tracked the Lagrangian float, with the exception of Underwater Vision Profiler (UVP) casts that were conducted both from the Process Ship and from the R/V *Ride* "Survey Ship" that transected the broader sampling region (Siegel et al., 2021). Measured in situ ocean current speeds and satellite-derived geostrophic velocities were used to model the advection of the salp bloom observed (see Section 2.5 below). During our study period OSP was characterized by a mean mixed layer depth of 29 m and mixed layer temperature of 14.1°C, a strong seasonal thermocline, mesopelagic temperatures ranging from 6°C at 100 to 4°C at 500 m, high surface macronutrients (8 μmol L^{-1} mixed layer nitrate + nitrite), and low chl a (~0.25 μg L^{-1} in surface) (Siegel et al., 2021). The base of the euphotic zone (1% surface PAR) averaged 78 m (range 70–90 m) (Siegel et al., 2021).

2.2. Animal Collection and Processing of Plankton Tows

Salps (which were exclusively the species *Salpa aspera*) and other zooplankton were collected from 0 to 1,000 m using a 1 m^2, 200 µm mesh Multiple Opening/Closing Net and Environmental Sensing System (MOCNESS, Wiebe et al., 1985), with the following discrete depth intervals sampled: 0–50, 50–100, 100–150, 150–200, 200–300, 300–400, 400–500, 500–750, and 750–1,000 m. The net was towed obliquely with a ship speed of 2 nm hr^{-1} and winch speed during sampling on the up-cast of 10–20 m min^{-1}. The total duration of each net deployment was 3.5–4.4 hr. Paired day-night tows (10:00–14:30 and 21:00–02:00 local time, respectively) were performed (sunrise ranged from 05:30 to 06:15; sunset from 19:00 to 20:00). A total of six day-night pairs of tows were completed, with one day-night pair at the beginning and end of each of the three epochs and associated sediment trap deployment periods.

Upon recovery, the MOCNESS nets were rinsed with seawater and the cod-ends were removed. Salps were removed from the tow and enumerated immediately, with displacement volume determined in graduated cylinders for the sum of all salps within each depth interval. The remainder of each net tow sample was then split using a Folsom plankton splitter and processed using protocols described in Steinberg et al. (2008). Half of the sample was size-fractionated using nested sieves, rinsed onto preweighed 0.2 mm Nitex mesh filters, and frozen at −20°C for biomass analysis. The other half sample was further split for additional analyses, with a portion preserved in sodium borate-buffered 4% formaldehyde for enumeration of major taxa (salps, copepods, amphipods, etc.) using an Olympus SZX 10 stereo dissecting microscope.

Throughout the cruise, additional tows to collect live salps and other zooplankton for experiments were performed within the upper 100 m using a 1-m diameter ring net (1,600-µm mesh for salps and some large copepods; 200 and 500-µm meshes for smaller taxa) with a nonfiltering cod end in short, vertical tows at low winch speed (10 m min^{-1}) to prevent damage to animals. Salps (and large copepods) were immediately transferred from vertical net tows performed within the upper 100 m using beakers or large ladles (wide-bore pipettes were used for smaller taxa) and into 20-L buckets containing surface mixed layer seawater (see below for description of individual experiments or measurements). Quantitative tows to measure salp abundance in the 100 m surface were also conducted at nighttime when salps were abundant. From these tows, animal lengths and total biovolume were measured.

2.3. Underwater Vision Profiler 5 (UVP) Imaging

The vertical distribution (0–1,000 m) of salps and their fecal pellets were also measured using high-definition versions of the Underwater Vision Profiler (UVP) (Picheral et al., 2010) mounted within the CTD-rosette on both the process and survey ships. Image acquisition was conducted on the downcast of each CTD profile (drop rate ~1 m s^{-1}) to map the distributions of salps and their fecal pellets. Each UVP illuminates and images a well-defined volume of water (1.06 and 1.13 L for the UVP on the Survey and Process ship, respectively) at a rate of approximately 6 Hz. Images of all particles and plankton with an equivalent spherical diameter (ESD) >500 µm were segmented and saved for later classification via the EcoTaxa online tool (Picheral et al., 2017). EcoTaxa built-in learning tools were used to predict the classification of each image, and these classifications were either individually corrected or validated by an expert. Because salps and their fecal pellets are relatively rare particles, UVP data from both Process and Survey ships were combined and binned into 10-m depth intervals to calculate volumetric concentrations (i.e., individuals or pellets m^{-3}). For salp fecal pellets, UVP data from the entire campaign were aggregated, whereas the salp data were separated by epoch for comparison with the MOCNESS tow data. We note that as the size of salps is large relative to the sampling volume of the UVP, and as salps imaged by the UVP were often part of a larger chain of multiple individuals not fully imaged in the sample volume, salp densities calculated from the UVP should be considered relative changes with depth rather than absolute density (see Table S1 in Supporting Information S1 for salp abundance calculated from net tows).

2.4. Biomass Analysis

Wet and dry weights for salps and other zooplankton were measured on a Sartorius BP211D or Mettler AE 160 balance. Wet weights were determined after samples were thawed on paper towels to remove excess water (~20 min). The samples were then dried for at least 24 hr at 60°C and reweighed. Wet and dry biomass per unit

volume (mg m^{-3}) was determined by dividing the biomass by seawater volume filtered through the net during sampling.

2.5. Advection Model

We used an advection model to predict the trajectory of the salp swarm, that is, where the salps observed during Epoch 1 went during Epochs 2 and 3, in order to assess if we were likely resampling the same salp patch throughout the cruise. A gridded velocity field (x, y, z, t) was developed from a combination of the measured currents from hull-mounted Acoustic Doppler Current Profiler (ADCP) instruments on both ships and satellite altimetry-derived geostrophic velocities (AVISO) (Estapa et al., 2021). The AVISO fields were used to provide spatial variability in the fields, with an attenuation in magnitude as a function of depth that was matched to the observed decay of the time-averaged velocities measured by the ADCPs. Temporal variation due to near-inertial, diurnal, and semidiurnal velocities was derived from high-pass filtered ADCP measurements and superimposed onto the AVISO-derived grid. The resulting velocity field had a resolution of 6 km grid scale and 15-min time intervals. We evaluated the skill of the predicted velocities by using a step-wise advection scheme to move virtual surface-tethered buoys and subsurface floats and then compared the predicted trajectories to the observed trajectories of the Lagrangian float, wirewalker, and surface-tethered sediment trap array. The model was confirmed to have very good predictive ability in the vicinity of the R/V *Revelle*—with modeled trajectories that diverged from the observed trajectories by an average of only 15 km over 8 days. Thus, we applied the same approach to predict the movements of the salp patch. At the MOCNESS start locations where salps were observed during Epoch 1, and starting at the beginning of the cruise (1 August), virtual salp particles were released and advected by the gridded velocity field. The particles were moved vertically within the water column, with a half-sinusoidal shape between 25 (night) and 500 m (day) that mimicked salp DVM behavior. The path of each modeled particle trajectory was then compared to positive observation of salps from net tows (MOCNESS tow from 0 to 1,000 m, or nighttime net tow within upper 0–100 m) and from the UVP. UVP data indicate the larger spatial extent and patchiness of the bloom, but were not collected simultaneously with net tows (so should not be used to directly compare with model results).

2.6. Fecal Pellet Production, Carbon Content, Sinking Velocity and Respiration Rate

The fecal pellet production by salps and other zooplankton was measured in shipboard experiments as described in Stamieszkin et al. (2021) for "individual species" experiments. Briefly, solitary and aggregate stage salps, copepods, amphipods, and euphausiids that were swimming and appeared in excellent condition were transferred from live net tow samples into experimental containers (20 L buckets for salps, 1 L containers for other zooplankton) filled with unfiltered surface seawater. After incubation at ambient surface temperatures for an average of ~5 hr (in the dark for salps and other zooplankton, plus at in situ mixed layer light conditions for other zooplankton), the animals were removed and frozen at −20°C. Fecal pellets were removed using a large-bore pipette (salps) or caught on fine mesh nitex screens (other zooplankton), counted, and measured under an Olympus SZX 10 stereo dissecting microscope at 12.5x (salps) or 63x (other zooplankton) magnification before being rinsed with DI water onto a precombusted GF/F filter and frozen at the same temperature. In the laboratory, animals were processed for biomass (as above) and both animals and their fecal pellets were analyzed for POC content as follows. Animals and pellets were dried at 60°C and after being weighed for dry mass, they were homogenized and placed into tin cups. Both the animal samples and pellets were fumed with hydrochloric acid to remove inorganic carbon and processed with a Costech 4010 Elemental Combustion System, yielding POC.

Carbon content of additional salp fecal pellets was measured on four 25 mm diameter precombusted quartz microfiber filters (QMA, nominal pore size 1 μm) containing four fecal pellets each. QMA filters were dried at 60°C and particulate carbon (PC) was measured on three filters and particulate inorganic carbon (PIC) measured on the fourth filter as described in Buesseler, Benitez-Nelson et al. (2020). Precombusted QMA filter blanks were measured for PC (4.8 μg C) and PIC (2.8 μg C). POC was obtained from the difference between blank-corrected PC and PIC results (PIC was ~4% of total PC).

Fecal pellet sinking velocities were measured on 22 individual salp fecal pellets in rotating tanks placed in a dark incubator set at in situ mesopelagic temperature (5°C). Pellets were collected from salps kept overnight in buckets, with some pellets aged for >1 day. Rolling tanks were filled bubble-free with ~1.2 L filtered seawater, a

single salp pellet was placed in each tank, and the rotation speed was adjusted depending on the size of the pellet (3.3–6.4 rpm). After 2–3 hr, when "solid body rotation" was established, the circular path of the fecal pellet in the tank was recorded and two replicate films of complete circles of each pellet analyzed to calculate sinking velocity from the orbital trajectories and the rotation speed of the tank (Ploug et al., 2010). Calculated replicate sinking velocities were on average ±2%, with two exceptions (±15%). Before and after sinking velocity determination, each pellet was photographed using a Carson® MM-840 eflex 75x/300x Digital Microscope system, and pellets were sized using the software GIMP 2.10.6. Width and length, and where possible depth, were determined for calculating fecal pellet volume. A mean depth of 25% pellet width was determined and used for all other calculations of fecal pellet volume herein. Comparison of preincubation and postincubation sizes indicated that pellets did not fragment during handling. Pellets were then transferred onto a combusted GF/F filter, acidified, and POC determined in a CEC44OHA elemental analyzer (Control equipment).

Microbial respiration rate of salp fecal pellets ($n = 7$) was measured at 5°C (mesopelagic temperature) using a microrespiration system (UNISENSE). The instrument was calibrated daily before measurements (with zero and 100% oxygenated water) and calibration and sample vials were submerged in a water bath held at constant temperature. After sizing (see above), individual pellets were transferred into a microchamber (700 µL) containing a stir bar and a screen separating the pellet from the stir bar. Stirring speed was set to 600 rpm. Oxygen measurements were conducted for three or four 10-min periods with 10-min breaks between each measurement period. Each measurement point was averaged over 10 s. The rate of change (linear) over the 1-hr measurement period was calculated and then each pellet was carefully transferred onto a combusted GF/F filter for POC determination as described for pellet sinking velocity.

2.7. Fecal Pellet Export

The export of salp fecal pellets was measured in polyacrylamide gel traps deployed on surface-tethered and neutrally buoyant sediment traps carrying collection tubes with jars containing a polyacrylamide gel layer (i.e., gel trap) deployed at the onset and recovered at the end of each sampling epoch (Durkin et al., 2021; Estapa et al., 2021). All sediment trap platforms additionally carried collector tubes containing 0.1% formaldehyde brine (70 ppt) for the preservation of bulk particulate fluxes. Details of trap deployments (Estapa et al., 2020), sample processing (Estapa et al., 2021), gel trap image analysis, and POC flux modeling by different particle types (Durkin et al., 2021) are presented elsewhere. Briefly, after recovery and at least 1 hr of settling time, samples were passed through 335 µm nylon screens, the screens were picked clean of zooplankton that had actively entered traps ("swimmers"), and then the remaining material was recombined with the <335 µm fraction. Samples were split on a custom rotary splitter (Lamborg et al., 2008), sample splits were filtered onto precombusted QMA filters, and PC and PIC were determined to obtain POC as described by Estapa et al. (2021). Sample composition and visual observation of filters indicated the presence of "swimmer" carbon in samples even after screening and picking; therefore, a subsequent correction of the POC flux was made using a statistical model based on sample composition and fluxes to gel traps (Estapa et al., 2021).

Gel traps were allowed to rest for at least one hour, then overlying seawater was removed, and micrographs of the particles within the gel were collected at four magnifications (7x, 20x, 50x, and 115x). An automated, python-based image processing protocol was used to detect and enumerate particles (Durkin et al., 2021). All detected particles were individually extracted from gel micrographs and manually classified, including salp pellets. Carbon content of classified particle types was modeled by estimating particle volumes from their two-dimensional surface area and converting them to carbon units (Durkin et al., 2021, https://github.com/cadurkin/Sediment_Trap_Gel_Image_Processing_2020). Salp pellet volumes were estimated as cuboids and widths were estimated by an empirically determined relationship with the measured ESD (width = 0.63 × ESD). Pellet depth was assumed to be 25% of the pellet width (see Section 2.6) and estimated volumes were multiplied by 0.04 mg C mm^{-3} to model carbon content (Durkin et al., 2021). This carbon conversion factor is larger than, but within one standard error of, mean C volume^{-1} determined from other salp fecal pellet data collected during the same cruise (0.01 ± 0.05 s.e.). The contribution of salp pellets to carbon flux was calculated by multiplying pellet carbon by their observed number flux in the traps (pellets m^{-2} d^{-1}). Total modeled carbon flux from particle images was calculated from all detected particle types to determine the relative contribution of salp pellets to total POC flux.

2.8. Active Transport by Diel Vertical Migration (DVM)

Active carbon transport by salps and mesozooplankton undergoing diel vertical migration (DVM) (mg C m^{-2} d^{-1}) included the respiration of CO_2, the excretion of dissolved organic carbon (DOC), fecal pellet egestion (POC), and predation mortality, while at depth during daylight hours (i.e., postgrazing in surface waters at night). Each of these parameters was calculated by applying published or measured metabolic allometric relationships to salp and other zooplankton biomass from MOCNESS tows (Maas et al., 2021) and based on a 14 hr occupation at depth each day by vertical migrators. Detailed methods for active transport calculations can be found in Supporting Information S1.

2.9. Carcass Export

The export of *Salpa aspera* carcasses after the demise of the bloom was calculated from daily mortality rates estimated as the proportion of the population reaching the end of its 15-day lifespan. This daily rate was applied to measured salp biomass in the top 100 m to calculate total carcass carbon export (Stone & Steinberg, 2016) using an average *Salpa aspera* carbon:dry weight ratio of 0.08 measured from salps used in fecal pellet production experiments (see Section 2.6). We assumed a life span of 15 days for this species based on salps of a similar size, including *Salpa fusiformis* (Deibel & Lowen, 2012; Henschke et al., 2011). Daily death rates were estimated as the proportion of the population reaching the end of its lifespan each day; thus, 1/15 (6.7%) of the *Salpa aspera* population dies each night. We note a second method of Wiebe et al. (1979) applied to a *Salpa aspera* bloom in the N. Atlantic assumed salps captured in the epipelagic zone during the day (which all appeared dead or moribund) died the night before—in that case 0.2%–0.4% of the nighttime biomass. As salps were sampled only during the day in epipelagic waters in one instance on our cruise, we used the life span calculation above. As the similarly sized salp species *Salpa fusiformis* sinks 700 m d^{-1} and decomposition is not rapid enough to significantly decrease biomass (Stone & Steinberg, 2016), we assumed 100% of the carcass biomass sank below 100 m. Carcass flux is based on life span (natural death), not predation mortality, and thus does not include consumption of sinking salp carcasses, which to our knowledge has not been measured, nor predation on live salps, for which there is evidence (Henschke et al., 2016) but also no rate measurements (and is already included in the active flux as an export term).

3. Results

3.1. Diel Vertical Migration and Swarm Advection

Depth-discrete, diel sampling from a multiple opening/closing net (MOCNESS) towed 0–1,000 m indicated that the salp population (exclusively *Salpa aspera*) was migrating from 300 to 750 m during the day into the upper 100 m at night (Figure 1), contributing to a >2-fold increase in total nighttime epipelagic zooplankton biomass due to DVM. When present, salps constitute 7%–56% of the total migrant biomass. Aggregated vertical profile data from the UVP show multiple peaks in the daytime abundance of salps occurring between 200 and 750 m, whereas the nighttime abundance was characterized by peaks in the epipelagic zone at (10–20 m) and at 50–70 m (Figure 1). Salp density in the upper 0–50 m (from MOCNESS tows) ranged from <0.01 to 0.38 individuals m^{-3} and from vertical tows in the upper 0–100 m (performed for live experiments) ranged from 0.06 to 1.9 individuals m^{-3} (Table S1 in Supporting Information S1). Salps were present in both aggregate (sexual) and solitary (asexual) stages, and many individuals of both stages contained one or more parasitic *Vibilia* spp. amphipods, which could also be seen in UVP images of salps in situ (Figures 2a–2c).

A salp advection model, which incorporated salp DVM behavior, was used to predict the trajectory of the salp swarm over the course of the study, which was conducted in three 8-day repeating Lagrangian sampling cycles or "epochs." The model predicted that the salps observed (in net tows) during Epoch 1 would drift north and veer eastward by Epoch 3 (Figure 3a). The "loops" in the trajectories are inertial circles that become more pronounced near the surface and diminish at depth due to DVM (Figure 3a). The salp trajectories predicted by the model generally followed the path of a subsurface (~95 m) Lagrangian float that was used to establish a frame of reference for the "Process Ship" sampling (see Section 2). The salp bloom was detected with UVP sampling by a second "Survey Ship" to the far reaches of our sampling area (i.e., >70 km across, Figure 3b), and while salp observations even within the swarm were patchy (salps were detected in 54% of UVP casts, Figure 3b), our results suggest that the same salp swarm was likely sampled throughout the cruise.
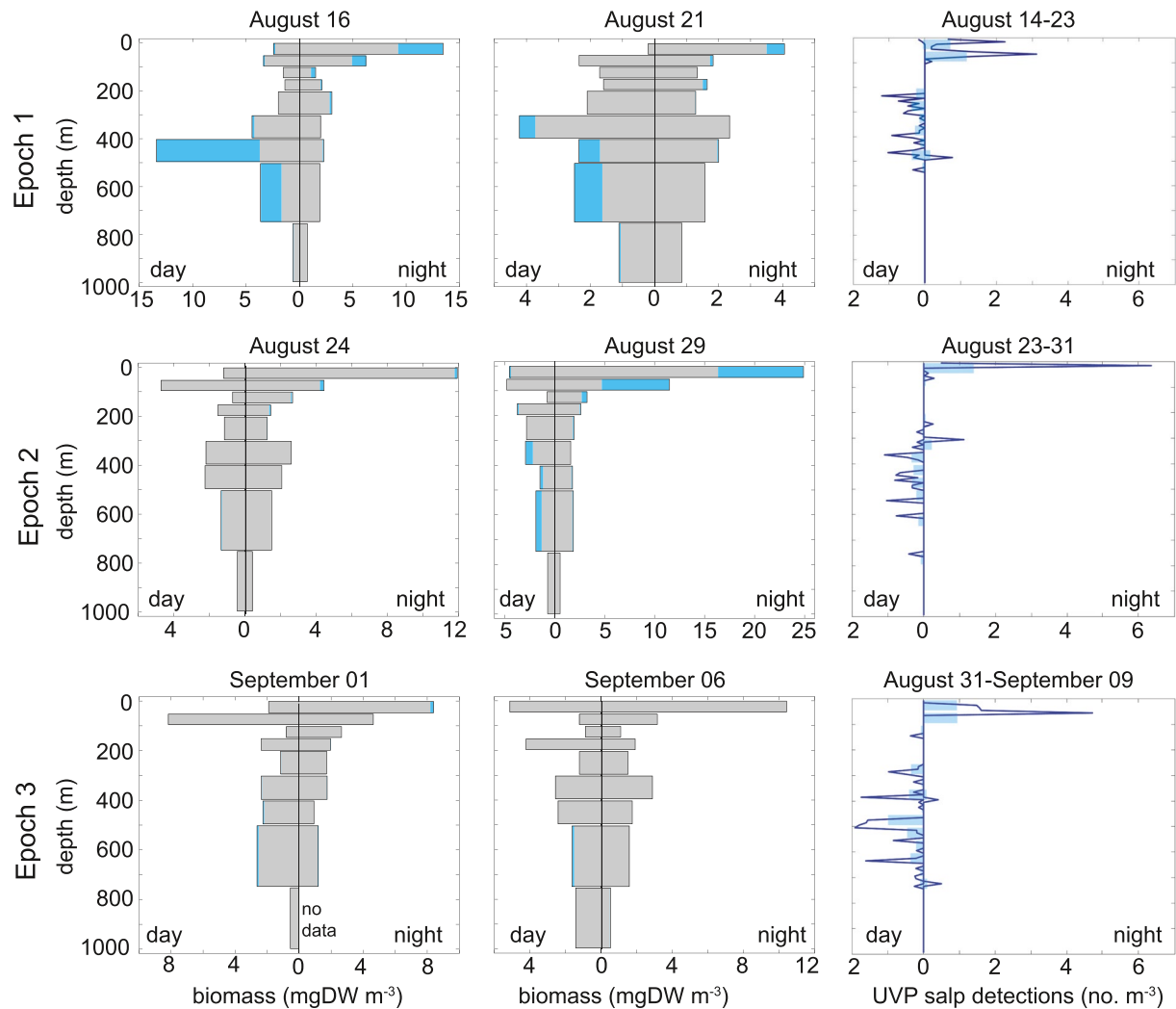
Figure 1. Depth distribution and diel vertical migration of salps. Discrete depth distribution of *Salpa aspera* during day and night as collected in Multiple Opening/Closing Net and Environmental Sensing System tows (blue) compared to mesozooplankton (zooplankton 0.2 to ~20 mm; light gray). Paired day and night tows were taken near the beginning and end of each of the three sampling epochs with start date of tows (month/day, 2019) shown for each pair. Note the biomass (*x*-axis) scales differ, and the irregular depth intervals reflecting the actual sampling intervals. The far right column shows the density of individual salps or salp chains detected in Underwater Vision Profiler (UVP) casts by epoch. UVP data are shown binned in 10 (line) and 50 m (bars) depth intervals and represent the mean vertical distributions of data aggregated across the entire study period and both the Survey and Process ships (see Section 2).

3.2. Fecal Pellet Production and Export

Salp fecal pellets ranged from <1 to 315 μg C pellet^{-1} and increased linearly with fecal pellet volume (Figure S1 in Supporting Information S1), with an overall mean of all measured salp pellets of 86 μg C pellet^{-1}. The fecal pellet production by individual salps in the epipelagic zone was on average ± SE 25.7 ± 14.0 μg C ind^{-1} h^{-1}, one to two orders of magnitude higher than crustacean taxa (amphipods, copepods, and euphausiids; 1.6 ± 0.8, 0.2 ± 0.1, and 0.1 ± 0.05 μg C ind^{-1} h^{-1}, respectively) (Figure 4a). Size-fractionated fecal pellet experiments indicate that salps accounted for up to 82% of the POC in fecal pellets produced by the whole zooplankton community (i.e., mesozooplankton plus salps) in the upper 100 m at night (Figure 4b). Sinking velocities of salp fecal pellets ranged from 441 to 1,345 m d^{-1}, with an overall mean of 779 m d^{-1}, and increased with increasing fecal pellet size (volume) (Figure S2 in Supporting Information S1). The microbial respiration rate on pellets was on average ± SE 0.6 ± 0.2 μg C pellet^{-1} day^{-1} ($n = 7$) at in situ mesopelagic temperatures, corresponding to 0.4% ± 0.03% of pellet C respired day^{-1}.

Daytime profiles of salp fecal pellets imaged by the UVP, averaged over the full study period, show that pellet concentrations in the upper 100 m (<0.2 m^{-3}) were lower compared to their concentrations in the mesopelagic
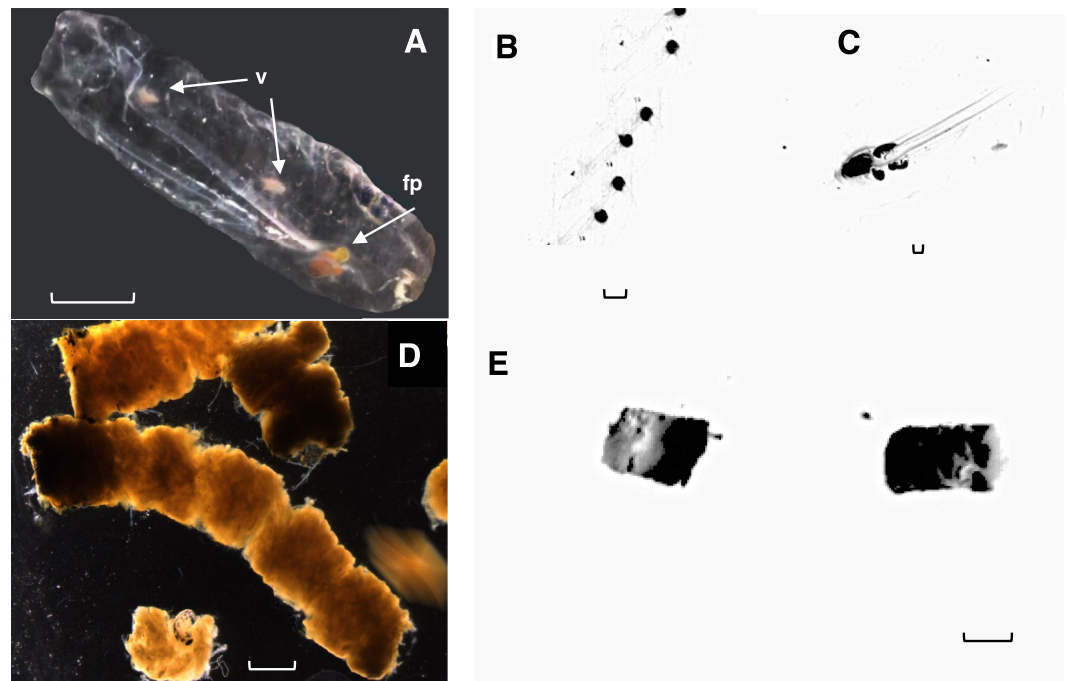
Figure 2. *Salpa aspera* and their fecal pellets. (a) *Salpa aspera* (solitary stage) collected in surface waters in net tows. Note parasitic *Vibilia* spp. amphipods (v) and a fecal pellet (fp) being produced to the right of the salp's gut. (b) *Salpa aspera* chain (aggregate stage) imaged by the Underwater Vision Profiler (UVP) at 498 m with individual salp guts visible as opaque spheres. (c) A solitary stage *Salpa aspera* parasitized by three *Vibilia* spp. amphipods imaged by the UVP at 47 m. (d) *Salpa aspera* fecal pellets collected aboard the ship during live salp incubations. (e) *Salpa aspera* fecal pellets imaged by the UVP at 759 (top) and 240 m (bottom). Scale bar for (a) is 2 cm and for (d) and all UVP images (b, c, and e) is 2 mm.

zone (0–0.6 m^{-3}), where pellets were present throughout the depth range sampled (Figure 4c). In contrast, the average salp fecal pellet concentration during the nighttime (0–0.9 pellets m^{-3}) was approximately double the daytime concentration throughout the water column, with a large peak occurring in the upper mesopelagic zone at 110–120 m. Other notable nighttime peak pellet densities occurred between 390–540 and 940–950 m (Figure 4c).

Salp fecal pellet export was high relative to the total POC flux measured in sediment trap gel collectors and comprised a patchy but significant proportion of total sinking POC (Figure 4d). Salp fecal pellet export was highest during Epoch 1 and lowest during Epoch 2. Mean salp fecal pellet export across the 100 m depth horizon was 15.8, <0.1, and 5.3 mg C m^{-2} day^{-1} during Epochs 1, 2, and 3, respectively; this was equivalent to 48.1%, 0.01%, and 14.9% of the respective modeled total 100 m POC flux. Salp fecal pellet export comprised an even higher proportion of the total POC export below 100 m, for example, during Epoch 1 comprising 88%, 85%, and 57% of modeled total POC flux at 208, 336, and 500 m, respectively (Figure 4d).

3.3. Active Transport

Salp active transport of C by DVM across 100 m totaled 1.0 mg C m^{-2} day^{-1} on average, and ranged from 0–4.1 mg C m^{-2} day^{-1} (Figure 5a, Table S2 in Supporting Information S1). The largest component of the total active flux by salps was respiratory CO$_2$ (55% of total, on average), followed by fecal pellet POC egestion at depth (19%), excretion of DOC (14%), and mortality due to predation (12%) at depth. Salp active flux was at times equivalent to >20% that of the entire migrating mesozooplankton community (e.g., 16 and 29 August), and at other times <5% of active flux was attributable to salps (Figure 5a, Table S2 in Supporting Information S1). Respiration was also the largest component of mesozooplankton total active flux (38%); mortality due to predation was similarly large (37%); and fecal pellet POC egestion at depth was the smallest component (12%) (in contrast to salps), with 13% due to mesozooplankton DOC excretion at depth (Figure 5b, Table S2 in Supporting Information S1).
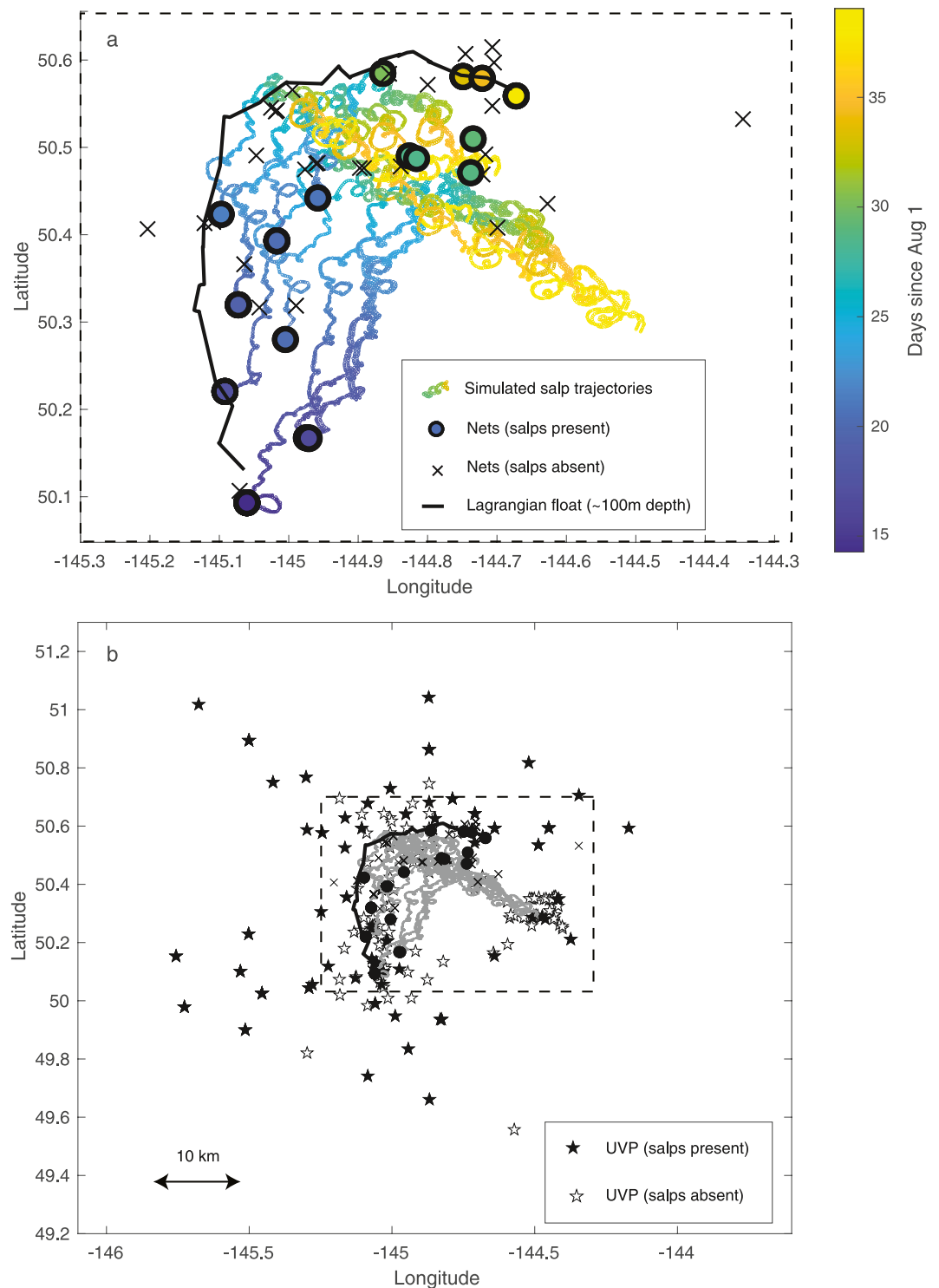
Figure 3. Salp advection model results compared to salps collected in net tows and placed in the larger spatial context of salp bloom as detected by the Underwater Vision Profiler (UVP). (a) Advection path of virtual salp particles. The colored lines show the lat-long path of that trajectory over the course of the sampling period (days since 1 August). Every time there was a positive observation of salps in a net tow, that symbol is colored with the time so it can be compared with the model. The X symbols indicate no salps were present in the net tow. Tow data are from the Process ship, which was following the Lagrangian float (black line). (b) Larger spatial context of the salp bloom as recorded by the UVP. Panel (a) is superimposed on salp presence/absence data from UVP casts from both the Survey ship and the Lagrangian Process ship.

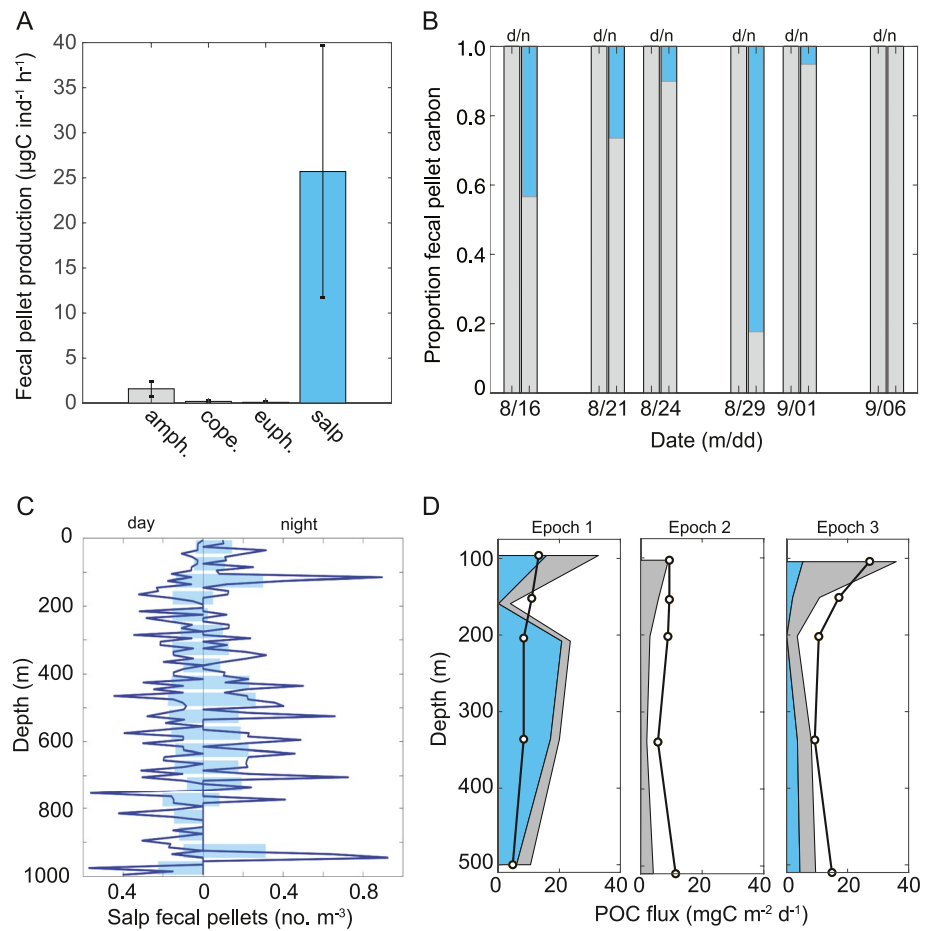**Figure 4.** Salp fecal pellet production and export. (a) Fecal pellet production in the epipelagic zone by *Salpa aspera* (blue) compared to abundant crustacean zooplankton taxa (light gray). Values are calculated from replicated experiments conducted during day and night for amphipods ($n = 6$ total experiments; replication within experiment ranged from 3 to 8 replicate experimental containers), copepods ($n = 9$), and euphausiids ($n = 3$), and at night for *S. aspera* ($n = 5$). (b) Contribution of *S. aspera* fecal pellet carbon production (blue) to total mesozooplankton community production (light gray) during day and night (d/n). (c) Depth profile of salp fecal pellets imaged by Underwater Vision Profiler (UVP) profiles during day and night (mean from entire study period). UVP data are shown binned in 10 (line) and 50 m (bars) depth intervals and represent the mean vertical distributions of data aggregated across the entire study period and both the Survey and Process ships (see Section 2). (d) Modeled export of salp fecal pellets (blue) from polyacrylamide gel traps compared to total particulate organic carbon (POC) export in sinking particles (gray). Line is measured, mean total POC flux from sediment traps; circles indicate the depth of trap collection. Values are averaged over each epoch. (a, b) Modified from Stamieszkin et al. (2021) and (d) from Durkin et al. (2021).

3.4. Sinking of Salp Carcasses

Carbon export potential from sinking salp carcasses from the top 100 m following the demise of this bloom averaged 0.9 mg C m^{-2} day^{-1}, and ranged from 0 to 4.3 mg C m^{-2} day^{-1}.

3.5. Comparison of Salp-Mediated Export Processes to Each Other and to POC Export Measured by Sediment Traps

The relative importance of salp-mediated export processes in the BCP at Station P is shown in Figure 6. On average, sinking salp fecal pellets (7.0 mg C m^{-2} day^{-1}) was the major salp export pathway (equivalent to 79% of all three salp export pathways combined), followed by sinking carcasses (0.9 mg C m^{-2} day^{-1}; 10% of total) and DVM active transport (1.0 mg C m^{-2} day^{-1}; 11% of total). Total mean salp-mediated export (8.9 mg C m^{-2} day^{-1}) was equivalent to 34% of the mean sinking POC flux across 100 m measured by sediment traps, with maximum total salp export (34 mg C m^{-2} day^{-1}) equivalent to 78% of maximum sediment trap flux (Figure 6).
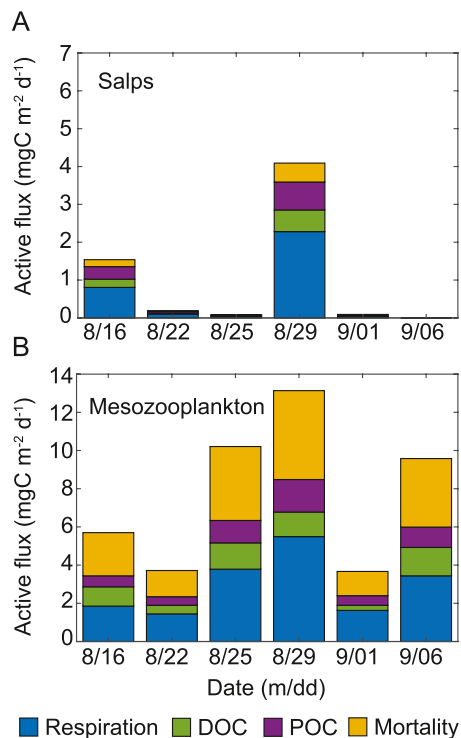
Figure 5. Active flux by diel vertical migration (DVM) of salps (*Salpa aspera*) compared to the mesozooplankton community. Total active flux via DVM consists of respiratory CO_2 (respiration), excreted dissolved organic carbon, and fecal pellets (particulate organic carbon) produced at a depth during the day after grazing in surface waters at night and mortality due to predation of vertical migrators at depth. (Mesozooplankton community represents all size classes 0.2 to ~20 mm, excluding salps).

4. Discussion

4.1. Overlooking Salps at Our Own Peril

Salp-mediated export processes were a major component of the BCP in late-summer at OSP, comparable to or exceeding (mostly crustacean) mesozooplankton-mediated export and usually dominating POC flux (comprised of phytoplankton aggregates, zooplankton fecal pellets, and other particles; Durkin et al., 2021) measured by sediment traps. The wide-ranging role salps play in carbon export is largely overlooked, or missed altogether, in less comprehensive field programs due to the ephemeral nature of salp swarms, their patchiness in space, DVM to less-frequently sampled meso-pelagic or deeper depths, and the exclusion of salp carcasses by sediment traps with baffles in their openings. Estapa et al. (2021) estimated collection probabilities of <5% for rare particles larger than 2 mm during the short trap deployments described here. A recent global carbon cycle model based on a global database of gelatinous zooplankton (cnidarians, cteno-phores, and pelagic tunicates—mostly salps) illustrates the global potential of salp-mediated export, but which is rarely measured (Luo et al., 2020). In this model, pelagic tunicate-mediated export comprised over three-quarters of the total gelatinous zooplankton POC export flux (carcass + fecal pellet export; DVM active flux was not modeled). Mean POC export by tunicates (2.7 Pg C yr^{-1}) was equivalent to 21%–67% of global POC export across 100 m (Luo et al., 2020) calculated based on global POC export ranging from 4 to 13 Pg C yr^{-1} (Dunne et al., 2007; Henson et al., 2011; Laws et al., 2000). Furthermore, the addition of pelagic tunicates into the Carbon, Ocean Biogeochemistry, and Lower Trophics version 2 global marine ecosystem model shunted carbon away from the microbial food web, shifting the overall balance of the oceans toward export and away from recycling (Luo et al., 2022). This single taxon thus has a remarkable capacity to enhance the BCP, especially in otherwise low-export, high recycling environments such as the HNLC subarctic Pacific.

4.2. Salps Increase Export and Efficiency of the Biological Carbon Pump in the HNLC Subarctic Pacific

The relative impact of salps on export and export efficiency is predictably high in oceanic regions such as the eastern subarctic Pacific, where iron limits diatom growth (e.g., Boyd et al., 2005) and the small phytoplankton that dominate are efficiently consumed by filter-feeding salps and exported in their rapidly sinking fecal pellets. HNLC regions have recently been identified in a global carbon model as "hotspots" where gelatinous zooplankton increase benthic transfer efficiency (largely via carcass sinking) beyond what is currently depicted in biogeochemical models, thus supporting benthic food webs (Luo et al., 2020). Salps are distributed throughout the eastern subarctic Pacific (Lüskow et al., 2022), and salp blooms have previously been reported during summer at OSP (*Cyclosalpa bakeri*—Madin & Purcell, 1992; Madin et al., 1997; Purcell & Madin, 1991; species unreported—Thibault et al., 1999), as well as in spring and summer over the more productive continental shelf and slope waters of the Gulf of Alaska (*Salpa aspera* and *C. bakeri*—Li et al., 2016). Salps occurred at OSP in June 2018 prior to our cruise where they, along with other pelagic tunicates, were suggested to contribute to high total organic carbon concentrations measured in the bathypelagic zone (Lopez et al., 2020). The presence of salps in the epipelagic zone at OSP is recorded as far back as the 1970s (Galbraith, 2021), and the Line P program zooplankton time series (1997 to present) indicates the regular occurrence of seasonal salp blooms, including *Salpa aspera*, at OSP (Figure 7), as also documented by Lüskow et al. (2022). A seasonal composite of this 23-year time series indicates peak salp abundance in June, when on average abundance is >2-fold in August and September—the season we sampled (Figure 7), suggesting that salp-mediated export is likely higher in late spring.

On a global scale, OSP is considered a low end member of BCP efficiency—a region with high euphotic zone recycling and low surface export, and high subsurface flux attenuation (Buesseler & Boyd, 2009; Siegel
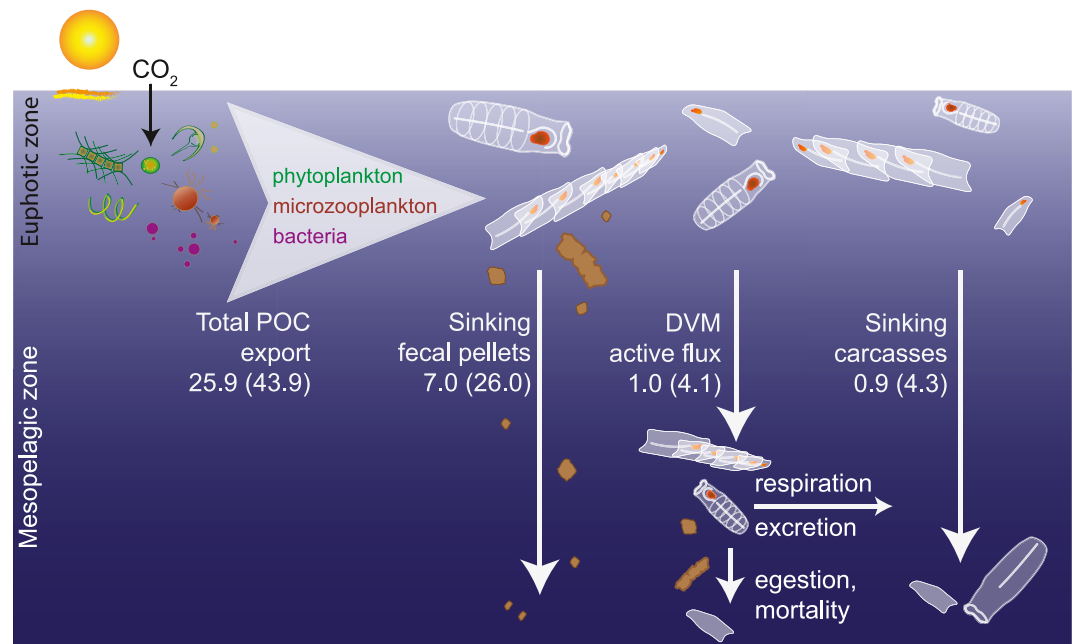
Figure 6. Relative importance of salp-mediated export processes in the biological carbon pump at Station P. Shown is mean (and maximum in parentheses) carbon export (mg C m^{-2} d^{-1}) across 100 m mediated by salp export processes compared to total particulate organic carbon (POC) export (passive sinking of particles from sediment traps as modeled from polyacrylamide gel traps, inclusive of salp fecal pellets). Inorganic carbon (CO_2) is fixed into POC by phytoplankton photosynthesis in surface and sunlit waters and incorporated into the microbial and plankton food web via a myriad of trophic interactions. Filter feeding salps consume a wide size range of plankton in surface waters, subsequently exporting this material using the processes quantified in this study: (a) passive sinking of POC as salp fecal pellets from the euphotic zone during feeding, (b) active flux by diel vertical migration (DVM)-consumption of POC in the euphotic zone at night and metabolism (respiration of CO_2, excretion of dissolved organic carbon, and egestion of POC as fecal pellets) and mortality in the mesopelagic zone during the day, and (c) passive sinking of POC as dead salp carcasses. See Table S2 in Supporting Information S1 for values of the individual components of the DVM active flux (also represented in Figure 5).
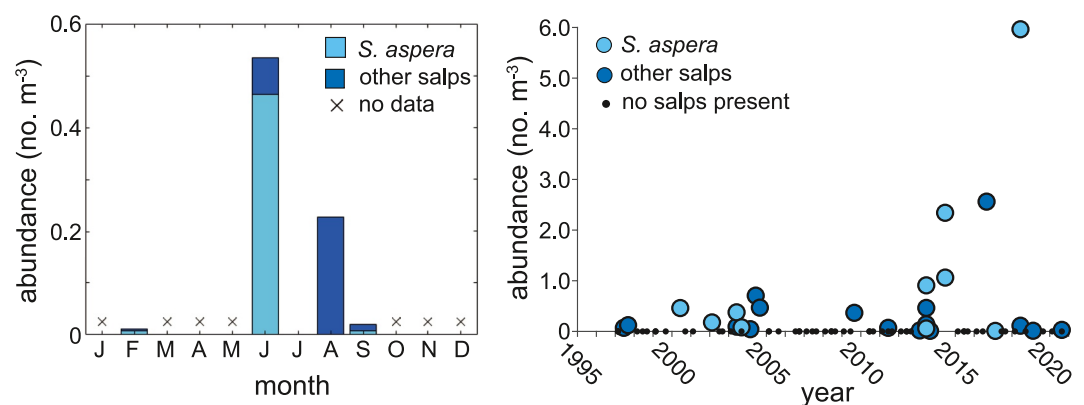

Figure 7. Salps (*Salpa aspera* and other salp species) in the upper 250 m at Ocean Station Papa (OSP), 1997 through 2020. (a) Seasonal composite representing mean of all samples taken during each month. Sample size for each month is $n = 24$ (February), 24 (June), 2 (July), 15 (August), and 10 (September); "*x*" indicates months in which no sampling occurred. (b) Salp abundance over time ($n = 75$); small black dots indicate samples taken with no salps. *S. aspera*, *Salpa aspera*; other salps, all other salp species combined (includes *Cyclosalpa bakeri*, *Salpa fusiformis*, *Salpa maxima*, plus unidentified species). Data are from the Line P time series, station P26 (OSP), where zooplankton were collected with bongo vertical net tows or MPS nets towed obliquely (200–250 μm mesh) within the upper 250 m. Shown are day and night data combined. Net tows were deployed at 0.5 and retrieved at 1 m sec^{-1}; a TSK flowmeter in the mouth of the net determined the volume of water filtered.

Table 1
Increase in Biological Carbon Pump Strength and Efficiency When Including Salp-Mediated Export

	Flux (mg C m^{-2} day^{-1})					
Depth	Trap POC	Salp FP	Trap POC (−salp FPs)	Salp DVM	Salp carcass	Total + salp export
100 m	25.9	7.05	18.9	1.0	0.9	27.8
200 m	10.0	6.95	3.1	1.0	0.9	11.9
	BCP metric	−Salp export				+Salp export
	E_z ratio	12%				18%
	T_{100}	16%				43%

Note. Shown are two metrics of the BCP: E_z ratio—the ratio of POC flux at the base of the euphotic zone (100 m) to net primary production (NPP)—is a measure of the strength of the BCP, while T_{100}—the ratio of the POC flux 100 m below the euphotic zone to the POC flux at the base of the euphotic zone (200 and 100m, respectively)—is a measure of BCP efficiency. Trap POC is the mean POC flux measured from polyacrylamide gel traps; Salp FP is salp fecal pellet flux; (−salp FPs) excludes salp fecal pellets; Salp DVM is active transport by diel vertical migration; Salp carcass is sinking of dead salps; Total + salp export is Trap POC (which includes salp fecal pellets) + Salp DVM + salp carcass. NPP was determined from ^{14}C incubations onboard, 156 mg C m^{-2} day^{-1}; data available at (https://seabass.gsfc.nasa.gov/archive/OSU/behrenfeld/EXPORTS/EXPORTSNP/archive). E_z ratio and T_{100} are compared for scenarios exclusive (−salp export) and inclusive (+salp export) of salp-mediated export. For example, E_z ratio (+salp export) is the ratio of Trap POC + Salp DVM + Salp carcass @100 m to NPP.

et al., 2016). The E_z ratio (ratio of POC flux at the base of the euphotic zone to NPP) is a measure of the strength of the BCP. During EXPORTS, the cruise-wide mean E_z ratio was 10%, 13%, and 17% (calculated using mean sediment trap fluxes at 100 m (Estapa et al., 2020), ^{234}Th-derived POC flux at 120 m (Buesseler, Benitez-Nelson et al., 2020), and modeled from polyacrylamide gel trap particle flux at 100 m (Durkin et al., 2021), respectively; NPP was determined from ^{14}C incubations onboard, 156 mg C m^{-2} day^{-1}). These measures of E_z ratio are conservative, as while POC export determined using traps or ^{234}Th already includes salp fecal pellet export, it excludes the respiratory component of salp active transport by DVM and largely excludes salp carcass sinking (Figure 6). Using mean values from Figure 6, and NPP above, including all salp-mediated export processes, increases the E_z ratio to 18%, which is 1.5-fold higher than the E_z ratio calculated excluding salp-mediated export of 12% (Table 1). Similarly, a recent study in the Southern Ocean found that the E_z ratio of 5%–10% in waters without salps increased to 42%–46% in waters with salps, due to the export of salp fecal pellets (Décima et al., 2022).

Salps also increased transfer efficiency at OSP, reducing attenuation of sinking organic matter with depth via remineralization by twilight zone zooplankton and bacteria (Giering et al., 2014; Steinberg et al., 2008). Salps contributed up to ∼80% of the total fecal pellet carbon produced by the entire zooplankton community at OSP. These large pellets sank rapidly, on average ∼780 m d^{-1}, and low remineralization rates of <1% of pellet C respired day^{-1} resulted in high salp fecal pellet POC export from the euphotic zone, as evidenced in both sediment traps and the presence of salp fecal pellets throughout the water column imaged by the UVP. The DVM behavior of *Salpa aspera* played a key role in enhancing transfer efficiency, as shown by the large peak in salp fecal pellets in the upper mesopelagic zone at night and doubling of salp fecal pellet concentration throughout the water column at night versus day. Vertically migrating salps egesting pellets at a depth after nighttime feeding in surface waters also accounted for the majority of the total carbon actively transported to depth.

Using the metric T_{100} (ratio of the POC flux 100 m below the E_z to the POC flux at the base of the E_z, including salp fecal pellets; Buesseler & Boyd, 2009), the transfer efficiency at OSP was 39%, 55%, and 60% (calculated using mean modeled flux from polyacrylamide gel traps at 100 and 200 m, Durkin et al., 2021; sediment trap fluxes at 100 and 200 m, Estapa et al., 2021; and ^{234}Th-derived POC flux at 120 and 220 m, Buesseler, Benitez-Nelson et al., 2020, respectively). Thus, 40%–61% of POC flux was remineralized in the upper twilight zone at OSP. Assuming that salp-mediated export by DVM active transport and carcass sinking surpasses 200 m with little to no attenuation (i.e., daytime migration depths always exceeded 200 m, and remineralization of large, fast-sinking carcasses is minimal), including all salp-mediated export processes increases T_{100} to 43%–60% (range using the three measures above), corresponding to decreased attenuation in the upper twilight zone of

40%–57%. Even more striking is that T_{100} inclusive of salp export (43%) is 2.6-fold higher than T_{100} excluding all salp-mediated export (16%) (Table 1).

4.3. Relative Importance of Salp-Mediated Export Processes

On average, salp-mediated export was equivalent to half that of the sinking POC flux across 100 m measured by sediment traps and at times exceeded trap flux. Sinking fecal pellets and active transport by DVM were the most important salp-mediated export processes, with passive sinking of salp carcass POC of lesser magnitude. A one-dimensional model of salp-mediated export processes in the Sargasso Sea, incorporating 17-year of salp abundance data, found salp-mediated export was equivalent to 11% on average, and a maximum of 60%, of total sinking POC flux measured by sediment traps at 200 m and exceeded the measured flux at 3,200 m (Stone & Steinberg, 2016). Similarly, in the Sargasso Sea, fecal pellet production was also the largest source of salp-mediated carbon flux, followed by DVM active transport, and with carcass sinking playing a minor role (Stone & Steinberg, 2016). In their global carbon cycle model, Luo et al. (2020) also found that of the gelatinous taxa, pelagic tunicates contributed the most to global POC export due to their high fecal pellet flux. Salp fecal pellets efficiently transport POC not only to mesopelagic depths as shown in our study, but contribute to deep carbon sequestration in the Northeast Pacific, where they have been recorded in meso- and abyssopelagic sediment traps (Matsueda et al., 1986; Wilson et al., 2013) and on the abyssal sea floor (Smith et al., 2014). Furthermore, in the Fe-limited NE Pacific, high grazing rates on phytoplankton and production of sinking fecal pellets by salps could contribute to further depletion of the dissolved Fe pool and Fe-limitation of primary production in surface waters. This has been posited for salp blooms in the HNLC Southern Ocean in a study that found high Fe content, low Fe release rates, and high export efficiency of *Salpa thompsoni* fecal pellets (Cabanes et al., 2017).

Salpa aspera underwent extensive daily vertical migrations and consequently active transport was a major component of salp-mediated flux. Many species of salps undergo DVM (Madin et al., 1996; Stone & Steinberg, 2014), and *Salpa aspera* blooms and DVM behavior have been well documented from the western North Atlantic, where this species also contributed substantially to fecal pellet carbon export (Madin et al., 2006; Wiebe et al., 1979). Vertically migrating pyrosomes (another order of pelagic tunicates) within a cold core eddy in the southwest Pacific actively transported 11 mg C m^{-2} d^{-1} below the mixed layer (Henschke et al., 2019) and in the NE Atlantic 2–65 mg C m^{-2} d^{-1} (Stenvers et al., 2021), indicating related taxa can also contribute significantly to export. Active transport specific to salps has only been reported once prior to our knowledge (Stone & Steinberg, 2016). Given that OSP salp-mediated active transport can exceed the entire rest of the migrating mesozooplankton community, active transport should be considered in future global models of salp (and other pelagic tunicate) export, and more broadly to reduce uncertainties in the BCP (Henson et al., 2022).

While carbon export from *Salpa aspera* carcasses played a lesser role overall compared to salp fecal pellet export and active transport by DVM, the magnitude of carcass export relative to other sinking particle fluxes was not trivial (equivalent to 9% of total sinking POC flux). Gelatinous zooplankton carcasses are an efficient transport mechanism of carbon to the deep sea (e.g., Lebrato et al., 2019), and salp carcass "jelly falls" have been reported on the deep seafloor where they provide food for benthic scavengers (Henschke et al., 2013; Smith et al., 2014). Fast sinking velocity and low decomposition rates allow much of the carcass carbon to be exported from the euphotic zone (Stone & Steinberg, 2016), making salp carcass export a potentially significant, albeit rarely quantified, export term. Consumption of sinking salp carcasses by mesopelagic scavengers or parasites is yet unquantified. The *Vibilia* spp. amphipods that we found commonly associated with *Salpa aspera* are, like other hyperiids, known salp parasites and can consume salp tissue (Gasca et al., 2015; Madin & Harbison, 1977) perhaps leading to flux attenuation.

5. Conclusion

Salps have unique and important effects on ocean biogeochemistry, and, especially in low flux settings, can dramatically increase the BCP efficiency and thus C sequestration. Despite the increasing realization of the key role that gelatinous zooplankton play in global carbon export, salps are mostly overlooked in less comprehensive field programs and models of the BCP. The challenge remains that salp blooms such as those we observed often go undetected, and the biogeochemical processes mediated by salps are rarely quantified, even in some of the best-studied regions of the world's oceans. Widespread future use of new technologies, such as adding video

imaging systems to autonomous profiling floats, would help detect these blooms. This study serves as a "call to arms" to better detect and quantify these processes, utilizing technology and sampling schemes that enable their inclusion in measurements and models of the BCP.

Data Availability Statement

Data for this project are available through NASA's SeaBASS data repository at https://seabass.gsfc.nasa.gov/experiment/EXPORTS (https://doi.org/10.5067/SeaBASS/EXPORTS/DATA001) and https://seabass.gsfc.nasa.gov/archive/VIMS/Steinberg/EXPORTS/EXPORTSNP/archive and in EcoTaxa at https://ecotaxa.obs-vlfr.fr. Specifically, taxon-specific fecal pellet production experiment data, which were also used in conjunction with biomass data to calculate salp fecal pellet contributions, can be found at https://oceandata.sci.gsfc.nasa.gov/ob/getfile/472d31b192_EXPORTS_NP_species_fecalpellet_production_experimental_R3.sb. Validation of the dissolved organic carbon and respiratory allometric equations is documented in Maas et al. (2021). The MOCNESS tow and zooplankton biomass data, used to determine depth-discrete, diel vertical distribution and calculate the active and passive flux of the mesozooplankton and salps can be found at https://oceandata.sci.gsfc.nasa.gov/ob/getfile/472d31b192_EXPORTS-EXPORTSNP_mocness_process_20191029_R3.sb. UVP data, which were used to determine patterns in salp and salp fecal pellet distribution can be found in EcoTaxa projects 1591 and 1286 at https://ecotaxa.obs-vlfr.fr/prj/1591 and https://ecotaxa.obs-vlfr.fr/prj/1286. Data and code associated with the advection model used to simulate the movement of the salp bloom are detailed in Estapa et al. (2021). Data and code associated with the image analysis of the gel traps is provided in Durkin et al. (2021).

References

Ahmad Ishak, N. H., Clementson, L. A., Eriksen, R. S., van den Enden, R. L., Williams, G. D., & Swadling, K. M. (2017). Gut contents and isotopic profiles of *Salpa fusiformis* and *Thalia democratica*. *Marine Biology*, *164*(6), 144. https://doi.org/10.1007/s00227-017-3174-1

Andersen, V. (1985). Filtration and ingestion rates of *Salpa fusiformis* Cuvier (Tunicata: Thaliacea): Effects of size, individual weight and algal concentration. *Journal of Experimental Marine Biology and Ecology*, *87*(1), 13–29. https://doi.org/10.1016/0022-0981(85)90188-1

Boyd, P. W., Strzepek, R., Takeda, S., Jackson, G., Wong, C. S., McKay, R. M., et al. (2005). The evolution and termination of an iron-induced mesoscale bloom in the northeast subarctic Pacific. *Limnology and Oceanography*, *50*(6), 1872–1886. https://doi.org/10.4319/lo.2005.50.6.1872

Bruland, K. W., & Silver, M. W. (1981). Sinking rates of fecal pellets from gelatinous zooplankton (salps, pteropods, doliolids). *Marine Biology*, *63*(3), 295–300. https://doi.org/10.1007/bf00395999

Buesseler, K. O., Benitez-Nelson, C. R., Roca-Martí, M., Wyatt, A. M., Resplandy, L., Clevenger, S. J., et al. (2020). High-resolution spatial and temporal measurements of particulate organic carbon flux using thorium-234 in the northeast Pacific Ocean during the EXport Processes in the Ocean from RemoTe Sensing field campaign. *Elementa: Science of the Anthropocene*, *8*(1), 030. https://doi.org/10.1525/elementa.030

Buesseler, K. O., & Boyd, P. W. (2009). Shedding light on processes that control particle export and flux attenuation in the twilight zone of the open ocean. *Limnology and Oceanography*, *54*(4), 1210–1232. https://doi.org/10.4319/lo.2009.54.4.1210

Buesseler, K. O., Boyd, P. W., Black, E. E., & Siegel, D. A. (2020). Metrics that matter for assessing the ocean biological carbon pump. *Proceedings of the National Academy of Sciences of the United States of America*, *117*(18), 9679–9687. https://doi.org/10.1073/pnas.1918114117

Cabanes, D. J., Norman, L., Santos-Echeandía, J., Iversen, M. H., Trimborn, S., Laglera, L. M., & Hassler, C. S. (2017). First evaluation of the role of salp fecal pellets on iron biogeochemistry. *Frontiers in Marine Science*, *3*, 289. https://doi.org/10.3389/fmars.2016.00289

Conroy, B. J., Steinberg, D. K., Stukel, M. R., Goes, J. I., & Coles, V. J. (2016). Meso-and microzooplankton grazing in the Amazon River plume and western tropical North Atlantic. *Limnology and Oceanography*, *61*(3), 825–840. https://doi.org/10.1002/lno.10261

Décima, M., Stukel, M. R., Nodder, S. D., Gutiérrez-Rodríguez, A., Selph, K. E., Lopes dos Santos, A., et al. (2022). Salp blooms increase carbon export 5-fold in the Southern Ocean. https://doi.org/10.1101/2022.02.07.479467

Deibel, D., & Lowen, B. (2012). A review of the life cycles and life-history adaptations of pelagic tunicates to environmental conditions. *ICES Journal of Marine Science*, *69*(3), 358–369. https://doi.org/10.1093/icesjms/fsr159

Deibel, D., & Paffenhöfer, G.-A. (2009). Predictability of patches of neritic salps and doliolids (Tunicata, Thaliacea). *Journal of Plankton Research*, *31*(12), 1571–1579. https://doi.org/10.1093/plankt/fbp091

Dunne, J. P., Sarmiento, J. L., & Gnanadesikan, A. (2007). A synthesis of global particle export from the surface ocean and cycling through the ocean interior and on the seafloor. *Global Biogeochemical Cycles*, *21*(4), GB4006. https://doi.org/10.1029/2006gb002907

Durkin, C. A., Buesseler, K. O., Cetinić, I., Estapa, M. L., Kelly, R. P., & Omand, M. (2021). A visual tour of carbon export by sinking particles. *Global Biogeochemical Cycles*, *35*(10), e2021GB006985. https://doi.org/10.1029/2021GB006985

Estapa, M., Valdes, J., Tradd, K., Sugar, J., Omand, M., & Buesseler, K. (2020). The neutrally buoyant sediment trap: Two decades of progress. *Journal of Atmospheric and Oceanic Technology*, *37*(6), 957–973. https://doi.org/10.1175/jtech-d-19-0118.1

Estapa, M., Buesseler, K. O., Durkin, C. A., Omand, M., Benitez-Nelson, C. R., Breves, E., et al. (2021). Biogenic sinking particle fluxes at Ocean Station Papa. *Elementa: Science of the Anthropocene*, *9*(1), 00122. https://doi.org/10.1525/elementa.2020.00122

Everett, J. D., Baird, M. E., & Suthers, I. M. (2011). Three-dimensional structure of a swarm of the salp *Thalia democratica* within a cold-core eddy off southeast Australia. *Journal of Geophysical Research*, *116*(C12), C12046. https://doi.org/10.1029/2011jc007310

Galbraith, M. D. (2021). DFO Pacific IOS zooplankton database - Line P. version 1. In *OBIS Canada Digital Collections*, Bedford Institute of Oceanography. Retrieved from http://ipt.iobis.org/obiscanada/resource?r=obis_dfo_ios_plankton_linep

Gasca, R., Hoover, R., & Haddock, S. H. (2015). New symbiotic associations of hyperiid amphipods (Peracarida) with gelatinous zooplankton in deep waters off California. *Journal of the Marine Biological Association of the United Kingdom*, *95*(3), 503–511. https://doi.org/10.1017/s0025315414001416

Giering, S. L., Sanders, R., Lampitt, R. S., Anderson, T. R., Tamburini, C., Boutrif, M., et al. (2014). Reconciliation of the carbon budget in the ocean's twilight zone. *Nature*, *507*(7493), 480–483. https://doi.org/10.1038/nature13123

Henschke, N., Bowden, D. A., Everett, J. D., Holmes, S. P., Kloser, R. J., Lee, R. W., & Suthers, I. M. (2013). Salp-falls in the Tasman Sea: A major food input to deep-sea benthos. *Marine Ecology Progress Series*, *491*, 165–175. https://doi.org/10.3354/meps10450

Henschke, N., Everett, J. D., Baird, M. E., Taylor, M. D., & Suthers, I. M. (2011). Distribution of life-history stages of the salp *Thalia democratica* in shelf waters during a spring bloom. *Marine Ecology Progress Series*, *430*, 49–62. https://doi.org/10.3354/meps09090

Henschke, N., Everett, J. D., Richardson, A. J., & Suthers, I. M. (2016). Rethinking the role of salps in the ocean. *Trends in Ecology & Evolution*, *31*(9), 720–733. https://doi.org/10.1016/j.tree.2016.06.007

Henschke, N., Pakhomov, E. A., Kwong, L. E., Everett, J. D., Laiolo, L., Coghlan, A. R., & Suthers, I. M. (2019). Large vertical migrations of *Pyrosoma atlanticum* play an important role in active carbon transport. *Journal of Geophysical Research: Biogeosciences*, *124*(5), 1056–1070. https://doi.org/10.1029/2018JG004918

Henson, S. A., Laufkötter, C., Leung, S., Giering, S. L. C., Palevsky, H. I., & Cavan, E. L. (2022). Uncertain response of ocean biological carbon export in a changing world. *Nature Geoscience*, *15*(4), 248–254. https://doi.org/10.1038/s41561-022-00927-0

Henson, S. A., Sanders, R., Madsen, E., Morris, P. J., Le Moigne, F., & Quartly, G. D. (2011). A reduced estimate of the strength of the ocean's biological carbon pump. *Geophysical Research Letters*, *38*(4), L04606. https://doi.org/10.1029/2011gl046735

Lamborg, C. H., Buesseler, K. O., Valdes, J., Bertrand, C. H., Bidigare, R., Manganini, S., et al. (2008). The flux of bio-and lithogenic material associated with sinking particles in the mesopelagic "twilight zone" of the northwest and North Central Pacific Ocean. *Deep Sea Research Part II: Topical Studies in Oceanography*, *55*(14–15), 1540–1563. https://doi.org/10.1016/j.dsr2.2008.04.011

Landry, M. R., Gifford, D. J., Kirchman, D. L., Wheeler, P. A., & Monger, B. C. (1993). Direct and indirect effects of grazing by *Neocalanus plumchrus* on plankton community dynamics in the subarctic Pacific. *Progress in Oceanography*, *32*(1–4), 239–258. https://doi.org/10.1016/0079-6611(93)90016-7

Landry, M. R., Monger, B. C., & Selph, K. E. (1993). Time-dependency of microzooplankton grazing and phytoplankton growth in the subarctic Pacific. *Progress in Oceanography*, *32*(1–4), 205–222. https://doi.org/10.1016/0079-6611(93)90014-5

Landry, M. R., Peterson, W. K., & Lorenzen, C. J. (1995). Zooplankton grazing, phytoplankton growth, and export flux: Inferences from chlorophyll tracer methods. *ICES Journal of Marine Science*, *52*(3–4), 337–345. https://doi.org/10.1016/1054-3139(95)80049-2

Laws, E. A., Falkowski, P. G., Smith, W. O., Ducklow, H., & McCarthy, J. J. (2000). Temperature effects on export production in the open ocean. *Global Biogeochemical Cycles*, *14*(4), 1231–1246. https://doi.org/10.1029/1999GB001229

Lebrato, M., Mendes, P. D. J., Steinberg, D. K., Cartes, J. E., Jones, B. M., Birsa, L. M., et al. (2013). Jelly biomass sinking speed reveals a fast carbon export mechanism. *Limnology and Oceanography*, *58*(3), 1113–1122. https://doi.org/10.4319/lo.2013.58.3.1113

Lebrato, M., Pahlow, M., Frost, J. R., Küter, M., de Jesus Mendes, P., Molinero, J.-C., & Oschlies, A. (2019). Sinking of gelatinous zooplankton biomass increases deep carbon transfer efficiency globally. *Global Biogeochemical Cycles*, *33*(12), 1764–1783. https://doi.org/10.1029/2019gb006265

Li, K., Doubleday, A. J., Galbraith, M. D., & Hopcroft, R. R. (2016). High abundance of salps in the coastal Gulf of Alaska during 2011: A first record of bloom occurrence for the northern Gulf. *Deep Sea Research Part II: Topical Studies in Oceanography*, *132*, 136–145. https://doi.org/10.1016/j.dsr2.2016.04.009

Longhurst, A. R., Bedo, A. W., Harrison, W. G., Head, E. J. H., & Sameoto, D. D. (1990). Vertical flux of respiratory carbon by oceanic diel migrant biota. *Deep-Sea Research, Part A: Oceanographic Research Papers*, *37*(4), 685–694. https://doi.org/10.1016/0198-0149(90)90098-g

Lopez, C. N., Robert, M., Galbraith, M., Bercovici, S. K., Orellana, M. V., & Hansell, D. A. (2020). High temporal variability of total organic carbon in the deep northeastern Pacific. *Frontiers of Earth Science*, *8*, 80. https://doi.org/10.3389/feart.2020.00080

Luo, J. Y., Condon, R. H., Stock, C. A., Duarte, C. M., Lucas, C. H., Pitt, K. A., & Cowen, R. K. (2020). Gelatinous zooplankton-mediated carbon flows in the global oceans: A data-driven modeling study. *Global Biogeochemical Cycles*, *34*(9), e2020GB006704. https://doi.org/10.1029/2020GB006704

Luo, J. Y., Stock, C. A., Henschke, N., Dunne, J. P., & O'Brien, T. D. (2022). Global ecological and biogeochemical impacts of pelagic tunicates. *Progress in Oceanography*, *205*, 102822. https://doi.org/10.1016/j.pocean.2022.102822

Lüskow, F., Galbraith, M. D., Kwong, L. E., & Pakhomov, E. A. (2022). Biology and distribution of salps in the subarctic Northeast Pacific. *Marine Biology*, *169*(6), 84. https://doi.org/10.1007/s00227-022-04067-2

Maas, A. E., Miccoli, A., Stamieszkin, K., Carlson, C. A., & Steinberg, D. K. (2021). Allometry and the calculation of zooplankton metabolism in the subarctic Northeast Pacific Ocean. *Journal of Plankton Research*, *43*(3), 413–427. https://doi.org/10.1093/plankt/fbab026

Madin, L. P., & Cetta, C. M. (1984). The use of gut fluorescence to estimate grazing by oceanic salps. *Journal of Plankton Research*, *6*(3), 475–492. https://doi.org/10.1093/plankt/6.3.475

Madin, L. P., & Deibel, D. (1998). Feeding and energetics of Thaliacea. In *The biology of pelagic tunicates* (pp. 81–103). Oxford University Press.

Madin, L. P., & Harbison, G. R. (1977). The associations of Amphipoda Hyperiidea with gelatinous zooplankton—I. Associations with Salpidae. *Deep Sea Research*, *24*(5), 449–463. https://doi.org/10.1016/0146-6291(77)90483-0

Madin, L. P., Kremer, P., & Hacker, S. (1996). Distribution and vertical migration of salps (Tunicata, Thaliacea) near Bermuda. *Journal of Plankton Research*, *18*(5), 747–755. https://doi.org/10.1093/plankt/18.5.747

Madin, L. P., Kremer, P., Wiebe, P. H., Purcell, J. E., Horgan, E. H., & Nemazie, D. A. (2006). Periodic swarms of the salp *Salpa aspera* in the Slope Water off the NE United States: Biovolume, vertical migration, grazing, and vertical flux. *Deep Sea Research Part I: Oceanographic Research Papers*, *53*(5), 804–819. https://doi.org/10.1016/j.dsr.2005.12.018

Madin, L. P., & Purcell, J. E. (1992). Feeding, metabolism. and growth of *Cyclosalpa bakeri* in the subarctic Pacific. *Limnology and Oceanography*, *37*(6), 1236–1251. https://doi.org/10.4319/lo.1992.37.6.1236

Madin, L. P., Purcell, J. E., & Miller, C. B. (1997). Abundance and grazing effects of *Cyclosalpa bakeri* in the subarctic Pacific. *Marine Ecology Progress Series*, *157*, 175–183. https://doi.org/10.3354/meps157175

Matsueda, H., Handa, N., Inoue, I., & Takano, H. (1986). Ecological significance of salp fecal pellets collected by sediment traps in the eastern North Pacific. *Marine Biology*, *91*(3), 421–431. https://doi.org/10.1007/bf00428636

Michaels, A. F., & Silver, M. W. (1988). Primary production, sinking fluxes and the microbial food web. *Deep-Sea Research, Part A: Oceanographic Research Papers*, *35*(4), 473–490. https://doi.org/10.1016/0198-0149(88)90126-4

Pfannkuche, O., & Lochte, K. (1993). Open ocean pelago-benthic coupling: Cyanobacteria as tracers of sedimenting salp faeces. *Deep Sea Research Part I: Oceanographic Research Papers*, *40*(4), 727–737. https://doi.org/10.1016/0967-0637(93)90068-e

Phillips, B., Kremer, P., & Madin, L. P. (2009). Defecation by *Salpa thompsoni* and its contribution to vertical flux in the Southern Ocean. *Marine Biology*, *156*(3), 455–467. https://doi.org/10.1007/s00227-008-1099-4

Picheral, M., Colin, S., & Irisson, J. O. (2017). EcoTaxa, a tool for the taxonomic classification of images. Retrieved from https://ecotaxa.obs-vlfr.fr

Picheral, M., Guidi, L., Stemmann, L., Karl, D. M., Iddaoud, G., & Gorsky, G. (2010). The Underwater Vision Profiler 5: An advanced instrument for high spatial resolution studies of particle size spectra and zooplankton. *Limnology and Oceanography: Methods*, *8*(9), 462–473. https://doi.org/10.4319/lom.2010.8.462

Ploug, H., Terbrüggen, A., Kaufmann, A., Wolf-Gladrow, D., & Passow, U. (2010). A novel method to measure particle sinking velocity in vitro, and its comparison to three other in vitro methods. *Limnology and Oceanography: Methods*, *8*(8), 386–393. https://doi.org/10.4319/lom.2010.8.386

Purcell, J. E., & Madin, L. P. (1991). Diel patterns of migration, feeding, and spawning by salps in the subarctic Pacific. *Marine Ecology Progress Series*, *73*, 211–217. https://doi.org/10.3354/meps073211

Siegel, D. A., Buesseler, K. O., Behrenfeld, M. J., Benitez-Nelson, C. R., Boss, E., Brzezinski, M. A., et al. (2016). Prediction of the export and fate of global ocean net primary production: The EXPORTS science plan. *Frontiers in Marine Science*, *3*, 22. https://doi.org/10.3389/fmars.2016.00022

Siegel, D. A., Cetinić, I., Graff, J. R., Lee, C. M., Nelson, N., Perry, M. J., et al. (2021). Overview of the EXport processes in the Ocean from RemoTe sensing (EXPORTS) northeast Pacific field deployment. *Elementa: Science of the Anthropocene*, *9*(1), 00107. https://doi.org/10.1525/elementa.2020.00107

Smith, J., Sherman, A. D., Huffard, C. L., McGill, P. R., Henthorn, R., Von Thun, S., et al. (2014). Large salp bloom export from the upper ocean and benthic community response in the abyssal northeast Pacific: Day to week resolution. *Limnology and Oceanography*, *59*(3), 745–757. https://doi.org/10.4319/lo.2014.59.3.0745

Stamieszkin, K., Steinberg, D. K., & Maas, A. E. (2021). Fecal pellet production by mesozooplankton in the subarctic Northeast Pacific Ocean. *Limnology and Oceanography*, *59*(7), 2585–2597. https://doi.org/10.1002/lno.11774

Steinberg, D. K., Mooy, B. A. S. V., Buesseler, K. O., Boyd, P. W., Kobari, T., & Karl, D. M. (2008). Bacterial vs. zooplankton control of sinking particle flux in the ocean's twilight zone. *Limnology and Oceanography*, *53*(4), 1327–1338. https://doi.org/10.4319/lo.2008.53.4.1327

Stenvers, V. I., Hauss, H., Osborn, K. J., Neitzel, P., Merten, V., Scheer, S., et al. (2021). Distribution, associations and role in the biological carbon pump of *Pyrosoma atlanticum* (Tunicata, Thaliacea) off Cabo Verde, NE Atlantic. *Scientific Reports*, *11*(1), 9231. https://doi.org/10.1038/s41598-021-88208-5

Stone, J. P., & Steinberg, D. K. (2014). Long-term time-series study of salp population dynamics in the Sargasso Sea. *Marine Ecology Progress Series*, *510*, 111–127. https://doi.org/10.3354/meps10985

Stone, J. P., & Steinberg, D. K. (2016). Salp contributions to vertical carbon flux in the Sargasso Sea. *Deep Sea Research Part I: Oceanographic Research Papers*, *113*, 90–100. https://doi.org/10.1016/j.dsr.2016.04.007

Stukel, M. R., Décima, M., Selph, K. E., & Gutiérrez-Rodríguez, A. (2021). Size-specific grazing and competitive interactions between large salps and protistan grazers. *Limnology and Oceanography*, *66*(6), 2521–2534. https://doi.org/10.1002/lno.11770

Stukel, M. R., Ohman, M. D., Benitez-Nelson, C. R., & Landry, M. R. (2013). Contributions of mesozooplankton to vertical carbon export in a coastal upwelling system. *Marine Ecology Progress Series*, *491*, 47–65. https://doi.org/10.3354/meps10453

Sutherland, K. R., Madin, L. P., & Stocker, R. (2010). Filtration of submicrometer particles by pelagic tunicates. *Proceedings of the National Academy of Sciences of the United States of America*, *107*(34), 15129–15134. https://doi.org/10.1073/pnas.1003599107

Thibault, D., Roy, S., Wong, C. S., & Bishop, J. K. (1999). The downward flux of biogenic material in the NE subarctic Pacific: Importance of algal sinking and mesozooplankton herbivory. *Deep Sea Research Part II: Topical Studies in Oceanography*, *46*(11), 2669–2697. https://doi.org/10.1016/S0967-0645(99)00080-6

Vargas, C. A., & Madin, L. P. (2004). Zooplankton feeding ecology: Clearance and ingestion rates of the salps *Thalia democratica*, *Cyclosalpa affinis* and *Salpa cylindrica* on naturally occurring particles in the Mid-Atlantic Bight. *Journal of Plankton Research*, *26*(7), 827–833. https://doi.org/10.1093/plankt/fbh068

Wassmann, P. (1997). Retention versus export food chains: Processes controlling sinking loss from marine pelagic systems. *Hydrobiologia*, *363*(1), 29–57. https://doi.org/10.1023/A:1003113403096

Wiebe, P. H., Madin, L. P., Haury, L. R., Harbison, G. R., & Philbin, L. M. (1979). Diel vertical migration by *Salpa aspera* and its potential for large-scale particulate organic matter transport to the deep-sea. *Marine Biology*, *53*(3), 249–255. https://doi.org/10.1007/BF00952433

Wiebe, P. H., Morton, A. W., Bradley, A. M., Backus, R. H., Craddock, J. E., Barber, V., et al. (1985). New development in the MOCNESS, an apparatus for sampling zooplankton and micronekton. *Marine Biology*, *87*(3), 313–323. https://doi.org/10.1007/BF00397811

Wilson, S. E., Ruhl, H. A., & Jr, K. L. S. (2013). Zooplankton fecal pellet flux in the abyssal northeast Pacific: A 15 year time-series study. *Limnology and Oceanography*, *58*(3), 881–892. https://doi.org/10.4319/lo.2013.58.3.0881